Energetic ion, atom, and molecule reactions and excitation in low-current H_2 discharges: Spatial distributions of emissions

Z. Lj. Petrović*
JILA, National Institute of Standards and Technology and University of Colorado, Boulder, Colorado 80309-0440, USA and Institute of Physics, University of Belgrade, P.O. Box 86, 11080 Zenum Belgrade, Serbia

A. V. Phelps†
JILA, National Institute of Standards and Technology and University of Colorado, Boulder, Colorado 80309-0440, USA
(Received 13 May 2009; published 17 July 2009)

Spatial distributions of H_α, H_β, and the near-uv continuum emission from the H_2 $a\ ^3\Sigma_g^+$ state are measured and compared with a model for low-current electrical discharges in H_2 at high E/N and low Nd, where E is the spatially uniform electric field, N is the gas density, and d is the electrode separation. Data are analyzed for 300 Td$<E/N<$45 kTd, $d=0.04$ m, and $2\times10^{21}<N<2.6\times10^{22}$ m^{-3}. (1 Td$=10^{-21}$ V m^2) The excitation is produced by electrons and by hydrogen atoms and molecules with mean energies from 5 to 1500 eV. Electron-induced emission, dominant at low E/N and low pressures, is distinguished by its buildup toward the anode. Excitation of H_α by fast H atoms dominates at high E/N and increases toward the cathode. The observed H_α emission at low E/N is normalized to previous experiments to yield absolute experimental excitation coefficients for all E/N and Nd. Small adjustments of model parameters yield good agreement with H_α data. Cross sections are derived for excitation of the H_2 near-uv continuum by H atoms. Spatial and pressure dependencies of H_α and H_2 near-uv emissions agree well with a model in which reactions of H_2^+, H_3^+, and H^+ ions with H_2 lead to fast H atoms and H_2 molecules, which then excite H atoms or H_2 molecules.

DOI: 10.1103/PhysRevE.80.016408 PACS number(s): 52.20.−j, 52.80.Dy, 34.50.Gb

I. INTRODUCTION

There has been renewed interest [1–9] in the processes occurring in low-current, uniform-electric-field, and low-pressure gas discharges in H_2. In this paper, we measure and compare with predictions the absolute magnitudes and spatial distributions of H_α and H_2 near-uv continuum emissions induced by electron, ion, atom, and molecule collisions with H_2. Thus, the present paper describes in detail one type of experiment briefly cited earlier [3] and uses these measurements to test the corresponding recent predictions of Ref. [10]. Additional experimental and modeling comparisons of Doppler broadened H_α line profiles [11] and of transient delays in currents and emission [12] test other aspects of the model [10]. The totality of the experiments and analyses demonstrate the usefulness of the model of the complex sequence of energetic hydrogen heavy-particle reactions with H_2 leading to H_α and H_2 near-uv continuum excitations. These successes suggest the usefulness of the description of the kinetics and transport for other weakly ionized hydrogen plasmas and its extension to partially dissociated hydrogen plasmas.

The reactive collision processes of importance in modeling the experiments of this paper are shown in the schematic of Fig. 1 of Ref [10]. This reference first updates the relevant cross sections for these processes. The paper then outlines a simplified solution utilizing multibeam flux and energy balance equations to calculate the spatial and the energy dependences of H^+, H_2^+, and H_3^+ ions and of fast H atoms and fast H_2 molecules. These fluxes and the relevant cross sections allow the calculation of the spatial dependence of emission for comparison with experiment in the present paper. Figures 7 and 8 of Ref. [10] illustrate the comparison of the model results with previously published [1] examples of data obtained in the present set of experiments. These data are included in the systematic studies of Sec. IV below.

Much of the recent work on low-pressure H_2 discharges has been motivated by plasma applications, such as semiconductor etching and sputtering deposition of materials [13] and by chemical analysis [14]. Of particular interest here are the experiments and analysis of ion and fast neutral behavior in the cathode fall of hydrogen discharges by Lauer *et al.* [15], Dexter *et al.* [16], Bretagne and co-workers [17], Heim and Störi [18], Bogaerts and Gijbels [14], Konjević and coworkers [19,20], and Babkina *et al.* [21]. These papers show the importance of fast H atoms and the conversion of H_2^+ to H_3^+, but there is disagreement [10,18,22] as to the importance of the breakup of H_3^+ in collisions with H_2. Here and in the remainder of this section, the references are chosen to illustrate the physics rather than to provide a historical development of the topic.

As work in our laboratory has shown for a number of gases [23–27], a useful indicator of heavy-particle excitation in a uniform-electric-field drift tube is a maximum in the emission near the cathode of a low-current high-voltage discharge instead of, or in addition to, the usual maximum in emission near the anode caused by electron avalanching and excitation. The first observation of a maximum in the emission near the cathode from a uniform-field drift tube appears to be that of Blasberg and de Hoog [28] during measurements of ionization coefficients for electrons in H_2 at low pressures. The pronounced maximum in H_β emission and a

*zoran.petrovic@phy.bg.ac.rs
†avp@jila.colorado.edu

weak maximum in molecular emission near the cathode depended on the cathode material and increased with increasing E/N. These authors suggested that electron nonequilibrium effects are responsible for the structure, but we argue that heavy-particle excitation is dominant. Ion energy distributions in low-current high-E/N discharges in H_2 have been briefly reported by Rao and co-workers [6,7]. Measurements and calculations of electron excitation coefficients for H_α and the near-uv continuum have been reported for uniform-field discharges by Petrović and co-workers [4,9,29]. Previous relevant models of discharges in H_2 are discussed in Ref. [10].

Intensity maxima have been observed close to the cathode in dc glow discharges in various gases [30,31]. They have been attributed to heavy-particle excitation or to the decrease in excitation cross section for very energetic electrons [30,32]. Evidence for H_α emission by fast H ($n=3$) atoms moving away from the cathode of a dc glow discharge [33–37] and from rf discharges [38,39] has been obtained from Doppler measurements. Barbeau and Jolly [37] attributed the production of fast excited H atoms in their dc glow discharge experiments in H_2 to excitation of fast ions and atoms on collision and reflection from the cathode. Our initial report of the present experiments [3] and Appendix B of Ref. [10] show that neither the surface excitation nor the decreasing electron excitation cross section models can account for the observed maximum near the drift-tube cathode in H_2. Reference [3] included the proposal that the observed heavy-particle excitation in H_2 near the cathode is primarily the result of H ($n=3$) excitation by fast H atoms produced in charge transfer collisions of H^+ with H_2 or by H atoms leaving the cathode. The present paper confirms the applicability of these proposals by providing a detailed comparison of a wide range of experiments with the model of Ref. [10].

The near-uv continuous spectrum of hydrogen has long been known to be excited by heavy particles [40], but the role of fast H atoms does not appear to have been determined. Chiplonkar [41] showed the similarity between the near-uv excited by hydrogen "canal rays" and that emitted by the hydrogen positive column, while Lunt *et al.* [42] determined the E/N dependence of electron excitation coefficients for the near uv for positive column E/N below 250 Td, where 1 Td$=10^{-21}$ V m^2. Legler [43] and Nygaard [44] obtained electron excitation coefficients for the far-uv emission for E/N below 750 Td. Stojanović *et al.* [29] measured absolute near-uv electron excitation coefficients using a drift tube for $200<E/N<6000$ Td.

An important part of the present paper is concerned with fast H atoms leaving the cathode as the result of bombardment by fast ions and neutral species. There is a considerable literature, motivated by plasma fusion experiments, giving the backscattered fraction and energy distribution of H atoms produced when H^+ ions and H atoms are incident on metallic and carbon surfaces [45–47]. These references show that both the "particle" and the "energy" reflection coefficients for H atoms from H^+ ions are significantly smaller for light atom targets than for heavy-atom targets. Experiments [3,19] have shown considerable variation in the relative efficiency of various discharge cathode materials for the excitation of H_α. The applicability of models predicting H-atom-induced excitation near discharge sheaths has been verified by measurements yielding the energy distribution of the H atom flux reflected from stainless steel [21]. Very recently, Cvetanović *et al.* [48] used Monte Carlo (MC) techniques to investigate the effects of various angular distributions of reflected atoms on the Doppler profiles observed normal to the scattering surface and parallel to the surface in glow discharges. Our initial report [3] summarizes observations of the Doppler effects associated with the reflected fast H atoms, but details are not yet published [11]. We report the details of those H_α emission measurements in which carbon in the form of graphite and a heavy-metal mixture of gold-palladium (AuPd) are used as cathodes subject to bombardment by hydrogen ions and atoms. This work provides evidence that the reflected fast H atoms are responsible for important components of the H_α emission [3].

In order to minimize the number of experimental parameters, the results in this paper are presented as functions of the reduced variables E/N and Nd (or pd, where p is the pressure) appropriate for moderate and low E/N drift-tube experiments and theory [30]. Experiments [49,50] and theory [51,52] show that these variables and the accompanying concept of electrons in "equilibrium" or a quasi-steady-state at the E/N are useful for describing electron behavior for $E/N\leq 700$ Td and $Nd\geq 10^{21}$ m^{-2}. The concept can be extended to lower Nd if one approximates the highly nonequilibrium region near the cathode by a delayed onset of ionization and excitation [10,30,49,53]. For typical H_2 densities, the mean particle energies for electrons at the anode and H^+ ions at the cathode [10] are 10 and 80 eV for $E/n=350$ Td. For $E/N=10$ kTd the electrons are close to free fall and the mean ion energy is ~400 eV. See further comments on the behavior of electrons and ions at very high E/N in Ref. [10].

Because of the complexity of the collisional kinetics in these experiments, it is recommended that the reader become familiar with at least Secs. II–IV of Ref. [10] before proceeding with the present paper. The apparatus and techniques used in these experiments with low-pressure H_2 discharges are discussed in Sec. II. Emission spectra for low and high E/N are presented in Sec. III. The measurements of the spatial and the pressure dependences of H_α emission are given and compared with the model in Sec. IV. Section IV C reports measurements for two cathode materials and for polarization of H_α. Measurements and modeling results for the near-uv continuum are presented in Sec. V.

II. EXPERIMENT

Figure 1 shows a schematic of the apparatus used for these and earlier experiments [54]. For a more detailed drawing of the drift tube, see Fig. 2 of Ref. [23]. The discharge tube consists of parallel-plane electrodes surrounded by a closely fitting fused silica cylinder [55] with O-ring sealed electrode mounts that can be baked at 100 °C. The fused silica cylinder and suitable feed-through insulators prevent long path breakdown and allow operation at pd on the left-hand side of the Paschen curve [30]. The high-voltage electrode is 7.8 cm in diameter, is made of vacuum grade sintered graphite [56], and serves as the anode, unless otherwise

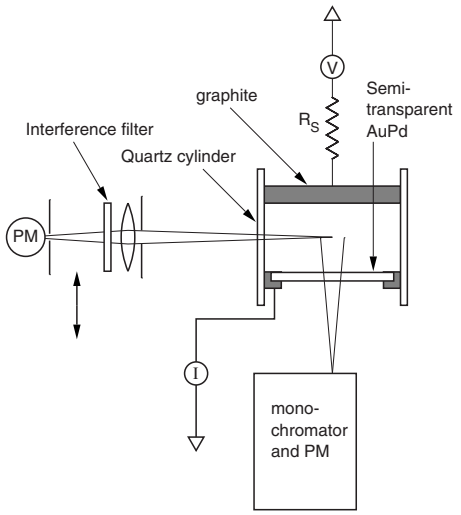

FIG. 1. Schematic of the drift tube, the photomultiplier, and the electrical circuit for the discharge.

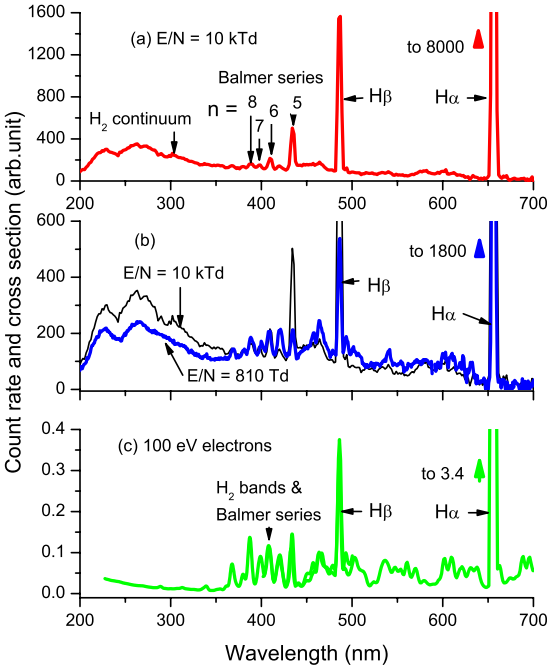

FIG. 2. (Color online) Representative spectral distributions for (a) for 10 kTd at 0.14 Torr and 1800 V, (b) E/N=810 Td at 0.3 Torr and 320 V, and (c) 100 eV electrons. The thick 810 Td curve in (b) is constructed from two different runs with a small overlap near 570 nm. The thin curve in (b) is copied from (a). The 100 eV electron curve in (c) is constructed from data from Refs. [64,65].

stated. The electrode at near ground potential is a semitransparent (~75% transmission) AuPd evaporated on to a quartz window. The semitransparent window is 6 cm in diameter and allows measurement of the discharge current and observation of the discharge emission parallel to the electric field. The spacing between electrodes is 4 cm. The high-voltage electrode does not have the Rogowski shape used previously [57] for operation at high pd, so that the maximum useful pd value is about 10 Torr cm (1 Torr=133 Pa). Reversal of the voltage connections to the electrodes allows us to study the effects of a graphite cathode material without baking the vacuum system and reconditioning the cathode. The emission count rates are normalized to the total discharge current at each spatial point, so that reasonably slow and small changes in discharge current can be tolerated, but we do require that the cathode be stable enough to allow a series of measurements at nearly constant discharge voltage ($\sim \pm 10$ V).

Most of the data were obtained using self-sustained discharges, where care is used to avoid oscillatory currents as detected with a 200 MHz storage oscilloscope [54]. Because of the stability limits [54], some of the pressure-dependent scans were obtained using a low-power mercury lamp [58] to produce photoelectrons that sustained the discharge. In these cases it is critical to subtract the signal at H_α wavelengths from mercury lamp light scattered by the electrodes, etc. The discharge current in our experiments is limited by an external resistor, typically 1 MΩ, between the high-voltage electrode and a stabilized voltage supply. The current is monitored and measured using an operational amplifier (>200 MHz) between the low-voltage electrode and the ground. This amplifier keeps the low-voltage electrode at close to the ground potential. The overall response of the current measurement is limited to ≥100 ns by cable capacitance and the sampling resistor. The self-sustained discharge operating voltage is essentially independent of current for the current densities used [54,59,60]. The voltages are measured to ±1% with a calibrated high-impedance voltmeter. The pressures are measured with a diaphragm manometer to a claimed accuracy of ±0.001 Torr and are room-temperature values (293 K). However, drift of the apparent pressure reading by ~2 mTorr was sometimes a problem. We will see that the H_α emission can be very sensitive to the discharge voltage and, especially, to the pressure.

The use of low currents prevents significant space-charge distortion of the approximately spatially uniform electric field and insures negligible nonlinear effects such as gas heating and collisions among excited and/or charged species. The discharges are operated at currents of less than 0.6 μA at all E/N. This corresponds to a current density of $<2 \times 10^{-4}$ A/m^2 and an estimated ion density of less than $\sim 10^{10}$ ions/m^3 or a fractional ionization of $<10^{-11}$. The estimated space-charge-induced change in electric field is negligible, i.e., about 1% of the applied field at our lowest E/N. The estimated fractional dissociation of the H_2 is $<10^{-8}$ and its effects are neglected.

The hydrogen is stated by the supplier to contain less than 10^{-5} impurities, so that for our experiments the principal contamination is from the rate of rise of pressure from leakage and/or outgassing for the sealed-off experiment of less than 10^{-2} Pa/min. Because of the low ionization potential of H_2 and H, charge transfer to impurities is not expected to be significant. Some evidence as to the gas purity is the absence of foreign gas spectra in Fig. 2. In these experiments we have not obtained highly reproducible cathode surfaces, such as those can be produced by extensive gas purification and by heavy sputtering and annealing [53,61]. The electrodes were chemically cleaned in an ultrasonic bath. After evacuation, the electrodes were mildly sputtered using a H_2 discharge for

~10 min at a current of less than ~1 mA, chosen to avoid constrictions and resultant nonuniformity of the cathode. Our cathode surfaces have light coatings of sputtered material, so that results may differ from those expected for clean materials [53]. Coatings of sputtered material on the quartz side wall are periodically removed to prevent optical loss. The gas temperature rise is negligible for the typical power input of less than 1 mW. Further details of the discharge tube, the vacuum conditions, the cathode treatment, and the pressure measurements are given in earlier papers [23,54,59].

Emission spectra in the wavelength range from 200 to 700 nm are obtained with a 1/4 m monochromator and Hamamatsu R928 photomultiplier. For the spectral scans, the monochromator was set for spectral resolution of ~4 nm at full width at half maximum (FWHM) and had a radial field of view at the discharge of about 10 mm. The spatial scans are obtained using a photomultiplier, an interference filter, a quartz lens, and a slit system mounted on a computer driven table that is scanned parallel to the axis of the drift tube as described previously [23]. The "high spatial resolution" slits described in Ref. [23] are used and yield approximately 1 mm resolution (FWHM). The H_α spatial scan is made using an interference filter centered at 656 nm with a FWHM of 11 nm and a selected and cooled Hamamatsu R928 photomultiplier. The H_β spatial scan is made with an interference filter centered at 485 nm with a FWHM of ~10 nm. The spatial scans for the H_2 near-uv continuum used a Hamamatsu R166 solar-blind photomultiplier sensitive from 160 to 320 nm with no added filter. The short-wavelength cutoff of ~200 nm for these uv spatial scans was determined by the "semiconductor" grade fused silica cylinder and fused silica lens. The short-wavelength cutoff of ~200 nm for the end-on spectral scans is determined by the photomultiplier, the monochromator and grating, and the fused silica cathode support and vacuum window used for observing the discharge.

III. SPECTRAL DEPENDENCE OF EMISSION

Representative scans of the spectral emission normalized to the discharge current as obtained looking along the discharge tube axis and parallel to the electric field are presented in Figs. 2(a) and 2(b). The curve in Fig. 2(a) is for $E/N=10$ kTd and 0.14 Torr. The wide curve in Fig. 2(b) is for $E/N=810$ Td and $p=0.32$ Torr and is obtained with the same detection sensitivity as the $E/N=10$ kTd data. These scans have been corrected for the manufacturer's spectral response of the photomultiplier, but not for the unknown response of the monochromator and grating. The curve in Fig. 2(c) shows our interpretation [62] of relative values for the measured excitation cross sections by 100 eV electrons [63–65] after adjustment for differences in instrumental resolution. The structure in our near-uv spectra near 240 nm and the decreased signal below 230 nm are not observed in the continuum observed and calculated by others [64,66,67] and are very probably instrumental effects.

Particularly noticeable in our spectral scans is the relatively large near-uv continuum intensity resulting from radiative transitions from the bound $a\ ^3\Sigma_g^+$ state to the unbound $b\ ^3\Sigma_u^+$ state. We also see the Balmer series and parts of several molecular bands resulting from transition between bound states of H_2. The data of Fig. 2 indicate that the discrete molecular band excitation relative to the Balmer series excitation, e.g., the H_β lines shown, is much lower for $E/N=10$ kTd than for 810 Td. A less obvious feature of Fig. 2 is that after background subtraction the available relative intensities of the Balmer series for all three excitation conditions vary approximately as n^{-6} for $2<n<6$. This correlation includes the directly measured relative cross sections for excitation of H ($n=2$, 3, and 4) in electron+H_2 collisions [64] and in H+H_2 collisions [68]. Also, all scans of Fig. 2 are consistent with the increase in excitation probability and the resultant possible production of a population inversion for $n=7$ and 8 found by James *et al.* [64] for electron excitation.

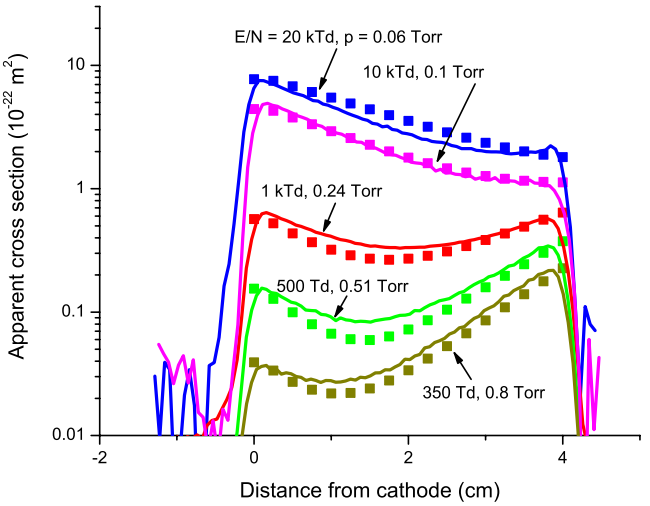

FIG. 3. (Color online) Absolute spatial distributions of apparent H_α emission cross sections for various E/N and pressures. The curves are calculated from the present measurements using the scale factor from Sec. IV A. The points are from the model of Ref. [10].

The model of Ref. [10], compared with experiment in the present paper, shows that excitation by fast H atoms causes about 85% of the production of H_α at $E/N=10$ kTd but accounts for only about 20% of the total at $E/N=800$ Td. The laboratory energy at the maximum of the H_α production by fast H is about 100 eV in both cases. This leads us to propose that the spectra shown in Fig. 2(a) are representative of excitation in H+H_2 collisions. Thus, H+H_2 collisions in the hundred eV range strongly favor excitation of the Balmer series and the near-uv band of H_2, but not the H_2 bands. The extension of excitation cross section measurements to the higher excited states of H and the near-uv continuum using beam techniques [68] would test these proposals. In this paper we will be principally interested in the H_α line and the $H_2 a\ ^3\Sigma_g^+ \rightarrow b\ ^3\Sigma_u^+$ near-uv continuum.

IV. SPATIAL DEPENDENCE OF H_α EMISSION

Examples of the very large changes in the magnitude and the spatial distributions of intensities observed for the H_α line are plotted in Fig. 3 for E/N values from 350 Td to 45 kTd at various pressures. These experimental data have been

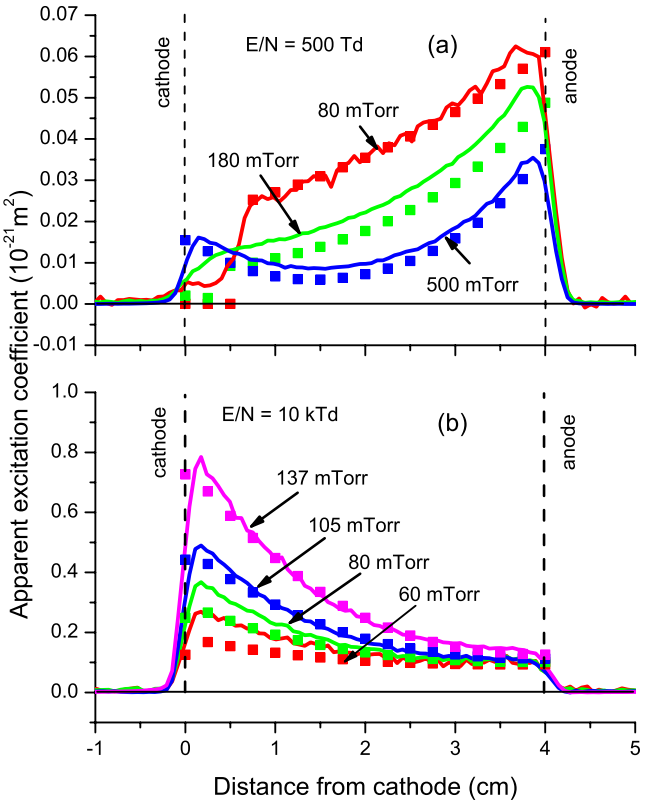

FIG. 4. (Color online) Representative spatial distributions of H_α emission for various pressures at (a) $E/N=500$ Td and (b) 10 kTd. The smooth curves are experiment and the points are from the model of Ref. [10].

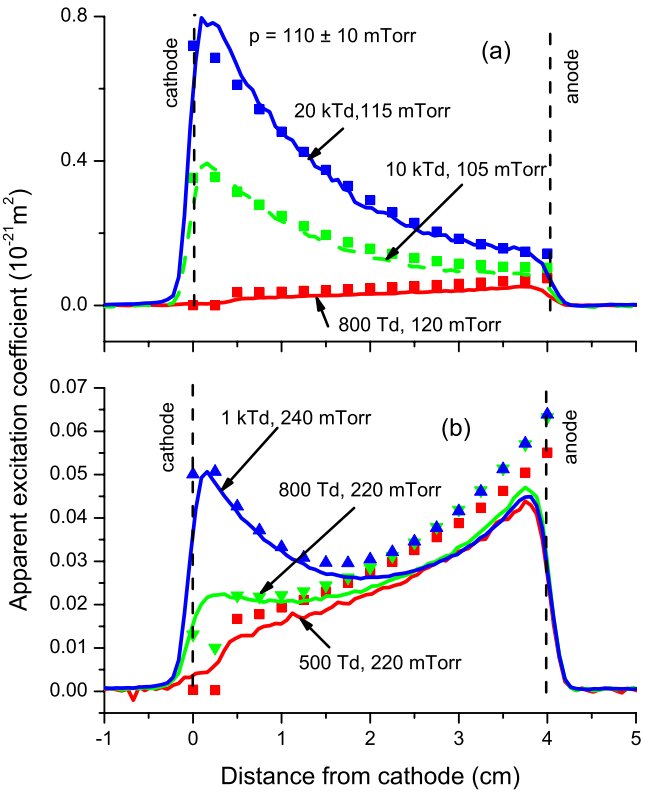

FIG. 5. (Color online) Representative spatial distributions of H_α emission for various E/N at constant pressure. (a) $p=0.11\pm0.01$ Torr and (b) $p=0.23\pm0.01$ Torr. The curves are from experiment and the points are from the model of Ref. [10].

made absolute as discussed in Sec. IV A. These apparent excitation cross sections are independent of discharge current to $\pm3\%$ for currents from 0.2 to 0.5 μA at $E/N=3$ kTd and $p=0.19$ Torr. Other tests [69] with D_2 show linearity of the emission to $\pm10\%$ from 0.5 to 10 μA. Having established the linearity of the emission with current, we next discuss the effects of discharge pressure and of E/N on the H_α line emission.

The changes in the spatial distributions of the apparent cross sections for H_α emission caused by changes in pressure at fixed E/N are shown in Fig. 4, while the effects of changes in E/N at fixed pressure are shown in Fig. 5. Data sets (not shown) showing a pressure dependence similar to that of Fig. 4(a) for $E/N=500$ Td are also obtained at 800 Td and 1 kTd. A data set (not shown) varying with pressure similar to that of Fig. 4(b) for 10 kTd is obtained at 20 kTd. The points shown in Figs. 4 and 5 are the predictions of the model of Ref. [10]. The comparisons of the model and the experiment are discussed further below.

From the spatial distributions of Fig. 4(a), one notes the relatively slow increase in H_α intensity near the anode with pressure at $E/N=500$ Td. On the other hand, the H_α intensity near the cathode increases much more rapidly than linearly with pressure at E/N of 500 Td and 10 kTd. We first analyze the peaks near the anode, which we attribute to excitation by electrons.

A. Absolute intensity of H_α emission

In this section, we utilize the well-understood [30] behavior of electron excitation and ionization at our low E/N to make a correction to the measured H_α emission for collisional quenching of H ($n=3$) atoms and to normalize the observed excitation data to an absolute scale. As found by several authors [28,50,70] and as expected from the Townsend theory of current growth [30,71], the optical emission from H_2 at $E/N\leq1000$ Td and sufficiently low pressures, increases exponentially with distance as one approaches the anode. Examples of such data are the curves of Fig. 4(a) for $E/N=500$ Td and the curves of Fig. 5(b) for $E/N\leq1$ kTd. The departure from exponential growth near the cathode at the lower pressures of Fig. 4(a) for $E/N=500$ Td is expected because of the distance required for the buildup of energy by the electrons leaving the cathode [30,49,50]. For the present, we ignore the peaks near the cathode for the higher-pressure data.

The spatial ionization (Townsend) coefficients derived by fitting an exponential growth to the emission data near the anode are shown by the triangles in Fig. 13 of Ref. [10]. The points for $E/N>600$ Td show a large spread in ionization coefficients determined from various experiments. This problem is considered further in connection with our current growth experiments [12].

As in our previous papers [3,23,24], we express the results of spatial scans in terms of the emission rate per unit

distance between the electrodes, i.e., the "apparent excitation coefficient" $\beta_x/N(z,E/N)$. This coefficient differs from the conventional Townsend-type coefficient [23,24,30] in that it is normalized to the total discharge current rather than to the local electron current. We do this because only in the case of emission data extrapolated to the anode at low E/N is the excitation expected to be limited to electron excitation and is the electron current equal to the measured total current [23]. Because of the low E/N and the moderate electron mean energies in these calibration experiments, electron reflection and ion emission from the anode can be neglected [23].

The signal recorded from the photomultiplier is proportional to the product of the discharge current i, the H_2 density, and the apparent excitation coefficient $\beta_x/N(z,E/N)$ and can be written as

$$S\{i,(E/N),N,z\} = C\frac{iN}{N_q}\frac{1}{(1+N/N_q)}\frac{\beta_x}{N}(z,E/N)$$
$$= \frac{Ci}{(1+N_q/N)}\frac{\beta_x}{N}(z,E/N). \quad (1)$$

Here we have assumed that the collisional quenching of H $(n=3)$ is accounted for by the factor $(1+N/N_q)^{-1}$, as obtained from the spatially independent solution to Eq. (B1) of Ref. [10] for the fraction of the excited atoms that radiate. We define the quenching density as $N_q=A/k_q$, where $A=0.98\times10^8$ s^{-1} is the effective radiative transition probability and k_q is the effective quenching rate coefficient [10].

If we apply Eq. (1) at the anode, $\beta_x/N(d,E/N)=\alpha_x/N(E/N)$ and

$$\frac{i}{S\{i,(E/N),N,d\}} = \frac{1}{C\alpha_x/N(E/N)}(1+N_q/N), \quad (2)$$

where $\alpha_x/N(E/N)$ is the Townsend-like coefficient for electron excitation of H_α. This result is in the Stern-Volmer form [72] and suggests the plot in Fig. 6 showing the reciprocal of the current-normalized count rate extrapolated to the anode versus the reciprocal of the H_2 density for various E/N. The straight line through the data for $E/N=500$ Td yields $N_q=(1.3\pm0.2)\times10^{22}$ m^{-3} and $C=(1.9\pm0.3)\times10^{33}$ counts s^{-1} m^{-2} A^{-1}, with an estimated accuracy of 15%.

Measurements of the quenching of H_α excitation [73–76] at room temperature using laser excitation led to quenching rate coefficients from 1.5×10^{-15} to 5×10^{-15} m^3/s. Using the statistically weighted radiative lifetime of the H $(n=3)$ state [77], our effective rate coefficient is $(5.0\pm0.8)\times10^{-15}$ m^3/s. The spread in coefficients may be the result of problems of interpretation of the data because of the effects of collisional and Stark mixing of the fine-structure levels [75,78]. The electric-field-induced Stark mixing [79] in our experiments is large and changes with pressure at fixed E/N. Measurements [80] at 10–35 keV energies suggest the quenching rate coefficient increases with excited atom velocity, but no data seem to be available for the 1–1000 eV energies of interest to us. We use the value of N_q derived above throughout this paper.

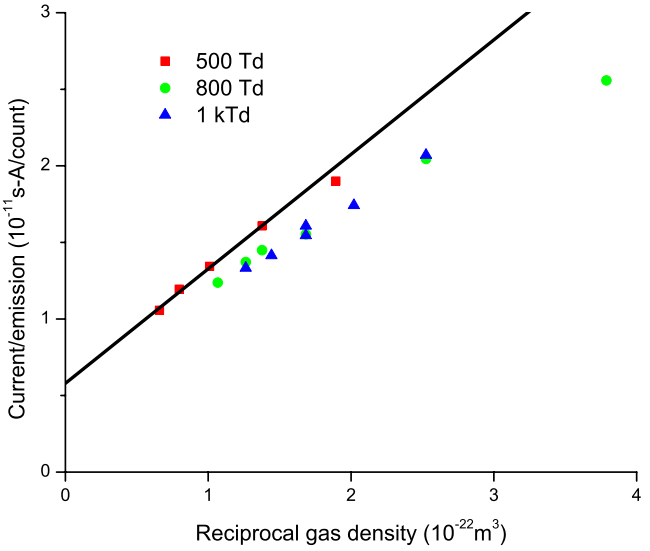

FIG. 6. (Color online) Reciprocal of measured H_α counting rates per unit discharge current extrapolated to anode versus reciprocal H_2 density.

B. Excitation by reflected atoms

Thus far, we have analyzed conditions such that the experimental H_α emission results from electron excitation of H_2 that increases exponentially toward the anode. More generally, the experiments show a second component of the H_α emission that increases toward the cathode. The ions and any fast neutral species that are produced by ions initially move toward the cathode. We proposed [3] that the second component is principally the result of heavy-particle excitation involving fast H atoms approaching and reflected from the cathode. In this section, we test this hypothesis by comparing the predictions of the model [3,10] for the spatially dependent H_α emission as one changes the contribution of the reflected atoms relative to the contribution of fast atoms approaching the cathode. Experimentally, we change the reflection properties of the cathode by simply reversing the sign of the potential applied to our drift tube equipped with different electrode materials. Here we have chosen the atomic mass of the two electrodes to be very different, e.g., AuPd versus carbon in the form of graphite.

Figure 7(a) shows the spatial dependence of H_α emission for an AuPd cathode and graphite anode (red) and for a graphite cathode and AuPd anode (blue). The measured spatial scan in the graphite cathode case has been reversed, so that the cathode is to the left in both cases. The small increase in E/N (≈15%) required for a self-sustained discharge with the graphite cathode indicates a lower electron yield per ion than for AuPd. The increased E/N is calculated [10] to result in an approximately 10% increase in the H_α excited by electrons. Instead, Fig. 7(a) shows an ≈30% decrease in the measured emission. As in Ref. [3], we propose that the decrease in H_α emission with the graphite cathode is the result of a lower number and lower energy of the H atoms leaving from graphite [45,47]. Figure 7(b) shows the predictions of the model of Ref. [10] calculated using reflection coefficient data from the literature [47] summarized in

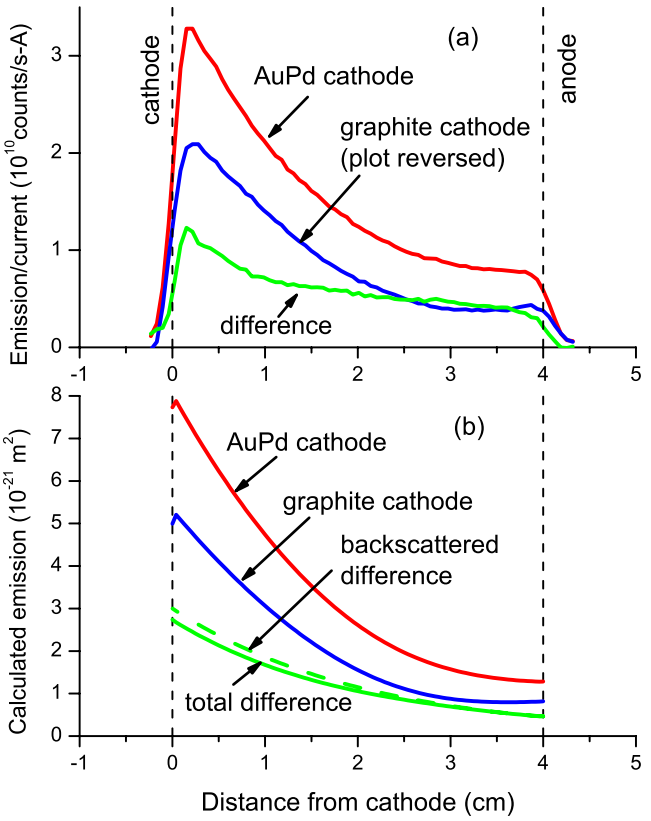

FIG. 7. (Color online) (a) Measured current-normalized H_α emission versus detector position for AuPd and graphite cathodes for $E/N=10\pm1$ kTd at $p=0.14$ Torr. The plot is reversed for the graphite cathode, so that the cathode is at the origin. (b) The predictions of the model of Ref. [10]. for the H_α emission with AuPd and graphite cathodes. The lower (green) curves compare the difference in calculated total emission for the two cathodes (solid curve) with the difference in H_α emission (dashed curve) produced by backscattered H atoms for the two cathodes.

Ref. [10]. The dependence of the H_α emission on the cathode material is characteristic of our low-current discharges [3] and of higher-current glow discharges [20,35] and is evidence that heavy-particle backscattering plays an important role in a wide range of discharges. Additional experimental and modeling support for this interpretation of the data of Fig. 7 is available from H_α Doppler emission profiles [3,11].

In order to obtain more detailed information regarding the components of the H_α excitation, the scans for the graphite cathodes are subtracted from these for the AuPd cathode in Figs. 7(a) and 7(b). Comparison of Fig. 7(a) with Fig. 7(b) shows a good agreement between the relatively slowly varying experimental difference and the difference in the total emission calculated [10] for backscattered fast H atoms. These differences also agree well with the calculated difference (dashed curve) between the excitations produced by the backscattered H atoms from the AuPd cathode and from the graphite cathode.

C. Balmer series and polarization

Figure 8 shows normalized spatial distributions of the emission of H_α and H_β for an E/N of 11 kTd. The spatial

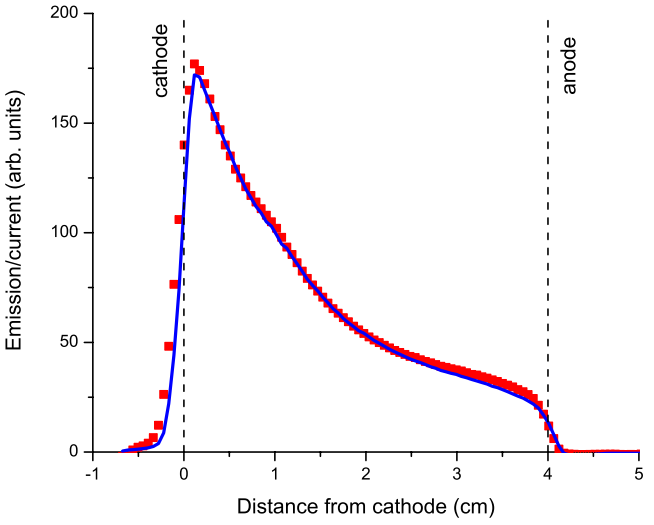

FIG. 8. (Color online) Normalized spatial distributions of H_α (points) and H_β (solid curve) for $E/N=11$ kTd.

dependences of these lines are nearly identical in spite the much larger quenching for the H ($n=4$) state than for H ($n=3$) [73]. These scans were obtained with different photomultiplier voltages, so that relative intensities are not known. The similarities of the spatial scans suggests that the excitation processes are the same for H_β as for H_α. This similarity of spatial distributions has also been found for D_α, D_β, and D_γ using this drift tube with D_2 [81] and for glow discharges in H_2 [20].

Measurements of the spatial dependence of the fractional polarization of the H_α emission were made so as to establish the nonisotropic nature of the exciting particles that produce the H_α emission. The data are obtained by placing a polarizer between the discharge and the interference filter and are shown in Fig. 9. The peak polarization is $\approx 8\%$ parallel the electric field at $E/N=10.4$ kTd, $p=0.15$ Torr, and $E=500$ V/cm. In the modeling paper [10] it is shown in Sec. IV B that the H_α excitation at this high E/N is primarily by fast H atoms. The measured polarization is approximately half the value found for this process using a beam of H atoms under single collision and negligible electric field conditions [68]. The lower observed polarization is qualitatively consistent with the approximately cosine distribution of H ($n=3$) velocities invoked in Sec. VB of Ref. [10] and in Refs. [11,48]. On the other hand, the observation of polarized H_α emission shows that the excitation is not produced by the isotropic H ($n=3$) atoms expected from some proposed schemes for H_α production in H_2 discharges [82]. The theory describing the effects of $3s$, $3p$, and $3d$ state mixing caused by our axial electric field have not been applied to the prediction of the polarization [79].

The measured polarization fraction decreases to $\approx(1\pm1)\%$ parallel the electric field at $E/N=1$ kTd, $p=0.45$ Torr, and $E=72$ V/cm. Because of the higher pressure and lower H atom energy, the H atoms responsible for this excitation are expected to be much more randomly directed than at $E/N=10$ kTd. Near the anode, the H_α excitation is by electrons, which produce a low maximum polarization [83]. At this E/N, the isotropic and the anisotropic

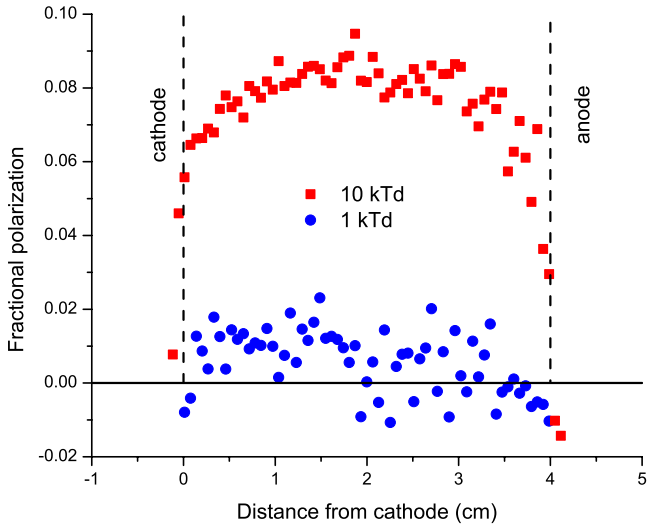

FIG. 9. (Color online) Measured fractional polarization of H_α for E/N of 1 kTd (blue circle points) and 10 kTd (red square points) versus distance from cathode. The small emission signals from outside the electrodes yield very erratic apparent polarization and are not shown.

components of the electron velocity distribution are expected to be comparable [84], leading to a further reduction in polarization. The large change in polarization as the E/N is reduced sets a limit on the false polarization introduced by our measuring system.

V. EXCITATION OF H_2 NEAR-UV CONTINUUM

Figure 10 shows spatially dependent excitation coefficients β/N for the near-uv continuum of H_2 for various E/N and H_2 pressures. These data are obtained without the use of a narrow band filter between the discharge and the solar-blind photomultiplier. Very similar data, but with much lower counting rate, are obtained using such a filter. Ionization coefficients obtained by fitting exponentials to such data in the vicinity of the anode are shown in Fig. 13 of Ref. [10] and, for unknown reasons, become as much as a factor of 2 higher at $E/N=3$ kTd than those obtained from H_α emission data. Just as for the H_α signals of Sec. IV, the absolute excitation coefficients are obtained by first extrapolating the count rates to the anode for a low E/N of 300 Td and various pressures. Using a plot similar to Fig. 6, the ratio of the intercept to the calculated and the measured [29,42] excitation coefficients shown in Fig. 13 of Ref. [10] gives the scale factor. Corrections for collisional quenching of the $H_2a\ ^3\Sigma_g^+$ state by H_2 are small [85,86]. It is important to keep in mind that this calibration procedure is independent of the unknown efficiency of the monochromator grating.

For the same E/N and pressure, the derived apparent excitation coefficients for the near-uv continuum of H_2 in Fig. 10 are much larger than the corresponding values for the H_α line shown in Figs. 4 and 5. These values and the higher quantum yield of the photomultiplier result in a much higher signal to noise ratio [87] for the near-uv spatial scans. The $H+H_2$ excitation cross section required to fit the measured

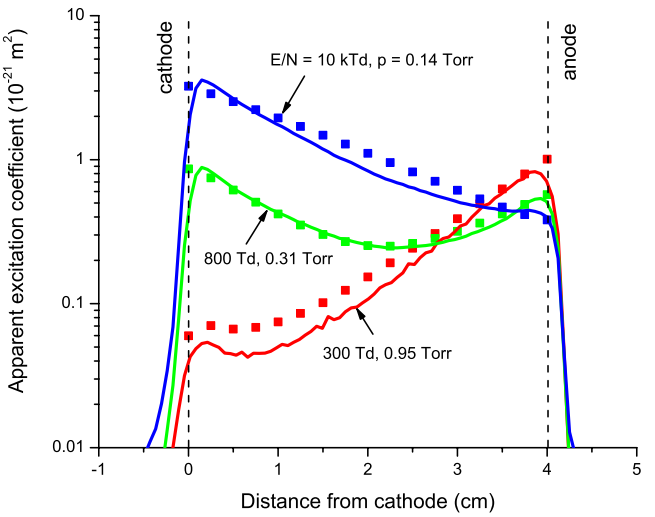

FIG. 10. (Color online) Representative spatial distributions of the H_2 near-uv continuum emission for various E/N. The solid curves are experiment and the points are the model results.

near-uv continuum signals is shown in Fig. 5 of Ref. [10]. This figure shows that at the lower energies the cross section for excitation of the near-uv continuum is significantly larger than that for H_α excitation.

There is a noticeable discrepancy between the calculated and the experimental heavy-particle excitation coefficients near the cathode shown for $E/N=300$ Td in Fig. 10. This difference would be reduced if the model used a "larger" ionization coefficient, α_i/N, with the resultant higher slope versus distance and a fixed intercept at the anode.

Evidence for the similarity of the excitation sequence for the near-uv continuum with that proposed for the H_α line is the similarity of the plots in Fig. 10 to those of Fig. 3 and the similarity of the fits of the calculated near-uv emission to experiment. The model indicates that the near-uv continuum for $E/N=10$ kTd and an AuPd film cathode is excited mostly by H atoms reflected from the cathode. The relatively slow decrease in near-uv emission with distance from the cathode in Fig. 10 in spite the short lifetime of the $H_2a\ ^3\Sigma_g^+$ state [85] ($\sim 10^{-8}$ s) is evidence against near-uv emission from excited H_2 produced in collisions of fast ions, atoms, or molecules with the cathode surface [37].

Spatially dependent emission data qualitatively similar to that of Figs. 3 and 10 have been obtained by Jelenković and Phelps [69] for the following D_2 transitions listed by filter wavelength and spectroscopic identification [88]: 250 ± 5 nm, $a\ ^3\Sigma \rightarrow b\ ^3\Sigma$; 610 ± 5 nm, $d\ ^3\Sigma \rightarrow a\ ^3\Sigma$; 402 ± 2 nm: $G\Sigma \rightarrow B^1\Sigma$; 836 ± 10 nm, $E^1\Sigma \rightarrow B^1\Sigma$; and 466 nm, $K^1\Sigma \rightarrow B^1\Sigma$. Spatial dependences of some of these transitions were obtained in H_2. Relatively low emission near the cathode resulting from heavy-particle excitation compared to the emission near the anode caused by electron excitation is particularly noticeable at $E/N \leq 2$ kTd. Such a behavior is expected on the basis of the relatively small discrete molecular bands found in the spectra for H_2 at high E/N in Sec. III.

VI. DISCUSSION

The preceding analyses of the strong spatial and pressure dependences of the H_α and the H_2 near-uv continuum emis-

sions show consistency of experiment with a model in which this emission is the result of a collision sequence that includes at several heavy-particle reactions. The model of Ref. [10] assumes that the reaction sequence begins with electron impact ionization to produce H_2^+. Eventually, the reactions produce fast H atom collisions and, to a lesser extent, fast H_2 molecule collisions with H_2 that excite the H atom or the H_2 molecule. At low E/N and relatively low mean heavy-particle energies, H_3^+ formation and breakup are important. At high E/N and higher mean particle energies, the breakup of H_2^+ is a key reaction. The spatial and the pressure dependences of H_α emission at high E/N is consistent with our previous proposal [3] of the importance of the reflection of hydrogen ions and neutrals from the cathode as fast H atoms that are subsequently excited in collisions with H_2. It should be kept in mind that the fit of the model to the absolute H_α emission experiments over a wide range of parameters presented in this paper is accomplished with no adjustments to the recommendations of Ref. [10] for the collisions cross sections of ions, atoms, and molecules with H_2. Some adjustment of the electron model is required and needs further investigation [12].

The consistency of our model and experiment for the observed spatial dependence of the near-uv continuum of H_2 is evidence that the same sequence of collision processes that produce the fast H atoms followed by H_α excitation also leads to excitation of the $a\ ^3\Sigma$ state of H_2 and the emission of the near-uv continuum of H_2. Because of the larger excitation cross sections for the near-uv continuum at lower collision energies than for H_α, the observation of this continuum may have relevance for hydrogen plasma diagnostics [66,89].

Because of the agreement of the experimental data with the model of electron excitation H_α near the anode at our low E/N, one is tempted to subtract off the exponentially growing electron component from the total emission and analyze the remaining heavy-particle excitation. Unfortunately, our cathodes have a sufficiently large reflection probability that the heavy-particle component of the emission is important. The resultant spatial dependence of the heavy-particle component obtained by subtraction contains comparable amounts of (a) the roughly exponential decrease with distance from the cathode caused by collisional and sidewall attenuation of the backscattered H atoms and of (b) the approximate power-law growth with distance from the anode expected for the multistep reaction sequence leading to fast H atoms and H_α excitation.

The deviations of the model results from experiment evident in Figs. 3–5 and in Fig. 10 may be the result of deficiencies in the simplified collision and numerical model presented in Ref. [10]. The multibeam solution could certainly be improved but gives consistency as the number of beams is increased from 1 [3] to near 100 [10]. The principal omission from the collision model is the neglect of angular scattering, i.e., the failure to take into account the generally unknown differential scattering cross sections for the various collisions. Models [9] using simplified differential scattering assumptions yield results in general agreement with the experiments of the present paper. The systematically lower than expected ionization and excitation coefficients derived from spatially dependent emission near the anode and discussed in Ref. [10] need further investigation, e.g., a search for a possible dependence of these experimental coefficients on discharge current and/or drift-tube geometry. Another concern is the accuracy of measurement of the lower pressures used at the higher E/N.

In parallel with the development of the multibeam solution to the kinetics model of Ref. [10] and the comparisons with the experiments described in the present paper and in Ref. [11], there has been the extension of MC techniques of Ref. [90] to the reactions and transport of ions, atoms, and molecules in H_2. Monte Carlo techniques allow one to predict the angular distributions of ions, atoms, and molecules and their effects on spatial distributions and, especially, on Doppler profiles [11]. Because of the lack of differential scattering cross section data for most of the collision processes [10], a set of very much simplified differential cross sections representing strongly forward scattering has been used in MC calculations. Also, changes in the angular integrated cross sections of Ref. [10] make comparisons of the MC and the multibeam solutions tentative. For the discharge condition of $E/N=10$ kTd and $p=0.14$ Torr, preliminary results using the MC technique shown in Fig. 4 of Ref. [91] yield spatial profiles very similar to the experimental and the multibeam results shown above in Fig. 4(b). The MC solution confirms the proposal of Ref. [3] that for the $E/N=10$ kTd case considered most of the H_α excitation is by fast H atoms backscattered from the heavy-metal cathode. The MC procedure also gives ion, atom, and molecule velocity distributions at different positions in the gap and, in the future, can be used to predict transient H_α emission and discharge current wave forms for comparison with experiment [12].

The present experiments point to the desirability of other measurements of spatially dependent H_α and H_2 continuum emission. For example, the use of a cathode made from a highly transparent grid, such as used for studies of heavy-particle excitation in Ar discharges [25,26], would greatly reduce the backscattered fast H atom flux. This would allow improved measurements of the spatial and the pressure dependences of emission produced by heavy particles, such as fast H and H_2, moving toward the cathode and provide a more detailed test of the reaction sequence of the excitation model.

Our spectral scans show a rather different distribution among the excited states of H_2 produced by fast H than when produced by 100 eV electrons. Although the H atoms and the H_2 molecules responsible for excitation at our high E/N have a wide range of kinetic energies, these heavy-particle collisions are observed to favor the production of lower excited states of H_2. The excitation of the near-uv continuum of H_2 by fast H has a particularly large probability at relatively low energies. These results point to the desirability of beam experiments and to the possibility of using this emission as a diagnostic for, as an example, aurora emission from the outer planets [92].

Several other experiments support the sequence of collision processes used to interpret our observations of the spatial dependence of emission in a low-current, low-

pressure, and high-E/N discharge. A recent experiment [21] has determined the energy distribution of H atoms produced by discharge ions striking a copper surface. The relatively large spatial extent of the H ($n=3$) excited atoms in our and other experiments supports our previous argument [3,10] that these excited atoms are not produced by collisions of fast particles with the cathode as proposed in Ref. [37]. At the calculated fast atom velocities, H_α produced by excited atoms formed at the cathode surface [93,94] would decay in distances on the order of millimeters, rather than the observed centimeters. The present results are strong evidence for atom and ion excitations as the source of the fast excited H atoms moving toward and away from the cathode in low-pressure dc and rf glow discharges [20,38,39,82]. In addition, measurements of spatial dependence of emission from the cathode fall region of dc discharges at much higher current densities are consistent with results of an extension of our uniform electric field model to the measured nonuniform electric field [20,26,95].

ACKNOWLEDGMENTS

We would like to acknowledge the contributions of B. M. Jelenković, who participated in closely related experiments. We benefited greatly from numerous helpful suggestions and the loan of equipment by A. Gallagher. We gratefully acknowledge J. D. Krakover, J. Feeney, R. Hart, T. Brown, and R. A. Mitchel for help with the personal computer and the electronics. The experimental work was supported in part by the Air Force Wright Laboratories, the National Institute of Standards and Technology, and the U.S.-Yugoslavia Joint Board Project No. 926. Preparation of this paper by A.V.P. was supported in part by JILA, while Z.Lj.P. was supported by the Ministry of Science of Serbia Project No. MNTRS141025.

[1] Z. Lj. Petrović and A. V. Phelps, in *Proceedings of the International Seminar on Reactive Plasmas*, edited by T. Goto (Nagoya University, Nagoya, 1991), p. 351.
[2] Z. Lj. Petrović, B. M. Jelenković, and A. V. Phelps, Bull. Am. Phys. Soc. **37**, 1951 (1992).
[3] Z. Lj. Petrović, B. M. Jelenković, and A. V. Phelps, Phys. Rev. Lett. **68**, 325 (1992).
[4] Z. Stokic, M. M. F. R. Fraga, J. Bozin, V. Stojanović, Z. Lj. Petrović, and B. M. Jelenković, Phys. Rev. A **45**, 7463 (1992).
[5] A. V. Phelps, Z. Lj. Petrović, and B. M. Jelenković, Bull. Am. Phys. Soc. **37**, 1966 (1992).
[6] M. V. V. S. Rao, R. J. Van Brunt, and J. K. Olthoff, in *Abstracts of International Symposium on Electron- and Photon-Molecule Collisions and Swarms*, edited by T. N. Rescigno, Berkeley, CA, 1995 (unpublished), p. H-9.
[7] J. Bretagne, G. Gousset, T. Šimko, M. V. V. S. Rao, R. J. Van Brunt, Y. Wang, J. K. Olthoff, B. L. Peko, and R. L. Champion, Europhys. Conf. Abstr. **20E**, 115 (1996).
[8] T. Šimko, V. Martišovitš, J. Bretagne, and G. Gousset, Phys. Rev. E **56**, 5908 (1997).
[9] Z. Lj. Petrović and V. Stojanović, Bull. Am. Phys. Soc. **51**, 64 (2006).
[10] A. V. Phelps, Phys. Rev. E **79**, 066401 (2009).
[11] The predictions of Ref. [10] for the Doppler broadening of the H_α line under conditions similar to those of the present paper have been found to agree well with experiment; Z. Lj. Petrović and A. V. Phelps (unpublished).
[12] Experimental transient current and H_α emission data for conditions similar to those of the present paper agree with qualitative predictions based on the model of Ref. [10]; Z. Lj. Petrović and A. V. Phelps (unpublished).
[13] M. A. Lieberman and A. J. Lichtenberg, *Principals of Plasma Discharges and Materials Processing* (Wiley, New York, 1994), Chap. 11.
[14] A. Bogaerts and R. Gijbels, Spectrochim. Acta, Part B **57**, 1071 (2002).
[15] E. J. Lauer, S. S. Yu, and D. M. Cox, Phys. Rev. A **23**, 2250 (1981).
[16] A. C. Dexter, T. Farrell, and M. I. Lees, J. Phys. D **22**, 413 (1989).
[17] J. Bretagne, G. Gousset, and T. Šimko, J. Phys. D **27**, 1866 (1994).
[18] D. Heim and H. Störi, J. Appl. Phys. **72**, 3330 (1992).
[19] M. R. Gemišić Adamov, M. M. Kuraica, and N. Konjević, Eur. Phys. J. D **28**, 393 (2004).
[20] N. Cvetanović, M. N. Kuraica, and N. Konjević, J. Appl. Phys. **97**, 033302 (2005).
[21] T. Babkina, T. Gans, and U. Czarnetzki, EPL **72**, 235 (2005).
[22] T. Šimko, J. Bretagne, and G. Gousset, in *Proceedings of the 23rd International Conference on Phenomena in Ionized Gases, Toulouse, France*, edited by M. C. Bordage and A. Gliezes (Université Paul Sabatier, Toulouse, 1997), p. II-184.
[23] B. M. Jelenković and A. V. Phelps, Phys. Rev. A **36**, 5310 (1987).
[24] A. V. Phelps and B. M. Jelenković, Phys. Rev. A **38**, 2975 (1988).
[25] D. A. Scott and A. V. Phelps, Phys. Rev. A **43**, 3043 (1991).
[26] Z. Lj. Petrović and V. D. Stojanović, J. Vac. Sci. Technol. A **16**, 329 (1998).
[27] B. M. Jelenković and A. V. Phelps, Phys. Rev. E **71**, 016410 (2005).
[28] H. A. M. Blasberg and F. J. de Hoog, Physica (Amsterdam) **54**, 468 (1971).
[29] V. Stojanović, J. Božin, Z. Stokić, Z. Lj. Petrović, and B. M. Jelenković, in *Proceedings of the Symposium on Atomic and Surface Physics, Obertraun, Austria*, edited by T. D. Mark and F. Howorka (Universität Innsbruck, Innsbruck, 1990), p. 160.
[30] M. J. Druyvesteyn and F. M. Penning, Rev. Mod. Phys. **12**, 87 (1940).
[31] K. Rózsa, A. Gallagher, and Z. Donkó, Phys. Rev. E **52**, 913 (1995).
[32] K. N. Ul'yanov, Zh. Tekh. Fiz. **40**, 2138 (1970) [Sov. Phys. Tech. Phys. **15**, 1667 (1971)].
[33] R. Döpel, Beitr. Plasmaphys. **16**, 411 (1976).

[34] W. Benesch and E. Li, Opt. Lett. **9**, 338 (1984).
[35] E. L. Ayers and W. Benesch, Phys. Rev. A **37**, 194 (1988).
[36] K. Prelec and Z. W. Šternberg, Fizika (Zagreb) **9**, 37 (1977).
[37] C. Barbeau and J. Jolly, J. Phys. D **23**, 1168 (1990).
[38] S. B. Radovanov, K. Dzierzęga, J. R. Roberts, and J. K. Olthoff, Appl. Phys. Lett. **66**, 2637 (1995).
[39] A. L. Cappelli, R. A. Gottscho, and T. A. Miller, Plasma Chem. Plasma Process. **5**, 317 (1985).
[40] J. Stark, Ann. Phys. **52**, 255 (1917).
[41] V. T. Chiplonkar, Proc. Natl. Inst. Sci. India, Part A **7**, 103 (1941).
[42] R. W. Lunt, C. A. Meek, and E. C. W. Smith, Proc. R. Soc. London, Ser. A **158**, 729 (1937).
[43] W. Legler, Z. Phys. **173**, 169 (1963).
[44] K. J. Nygaard, J. Appl. Phys. **36**, 743 (1965).
[45] G. M. McCracken, Rep. Prog. Phys. **38**, 241 (1975).
[46] W. Eckstein and H. Verbeek, in *Data Compendium for Plasma-Surface Interactions*, edited by R. A. Langley *et al.* (International Atomic Energy Agency, Vienna, 1984), p. 12.
[47] R. Aratari and W. Eckstein, Nucl. Instrum. Methods Phys. Res. B **42**, 11 (1989).
[48] N. Cvetanović, B. M. Obradović, and M. M. Kuraica, J. Appl. Phys. **105**, 043306 (2009).
[49] M. A. Folkhard and S. C. Haydon, Aust. J. Phys. **23**, 847 (1970); **24**, 519 (1971); **24**, 527 (1971).
[50] A. B. Wedding, H. A. Blevin, and J. Fletcher, Aust. J. Phys. **18**, 2361 (1985).
[51] H. A. Blevin, J. Fletcher, and S. R. Hunter, J. Phys. D **11**, 1653 (1978).
[52] M. S. Mokrov and Yu. P. Raizer, Zh. Tekh. Fiz. **78**, 47 (2008) [Tech. Phys. **53**, 436 (2008)].
[53] A. V. Phelps and Z. Lj. Petrović, Plasma Sources Sci. Technol. **8**, R21 (1999).
[54] Z. Lj. Petrović and A. V. Phelps, Phys. Rev. E **47**, 2806 (1993).
[55] Semiconductor grade fused silica.
[56] Vacuum grade POCO graphite, Poco Graphite, Inc., 300 Old Greenwood Road, Decatur, Texas 76234, USA.
[57] S. A. Lawton and A. V. Phelps, J. Chem. Phys. **69**, 1055 (1978).
[58] "Pen-Ray" lamp, UVP Inc., 2066 West 11th Street, Upland, California 91786, USA.
[59] B. M. Jelenković, K. Rózsa, and A. V. Phelps, Phys. Rev. E **47**, 2816 (1993).
[60] A. V. Phelps, Z. Lj. Petrović, and B. M. Jelenković, Phys. Rev. E **47**, 2825 (1993).
[61] F. M. Penning and J. H. A. Moubis, Philips Res. Rep. **1**, 119 (1946); Physica (Utrecht) **15**, 721 (1949).
[62] The data are obtained by automatically digitizing published graphs from Refs. [64,65]. As a result, there is a considerable uncertainty in the resultant numerical values used as an input for our analysis. The relatively high-resolution data of their figures have been folded into our instrument function and so reduce the bias between the peak magnitudes of the near-uv continuum relative to the narrow Balmer series lines to values of our experiments. The relative areas under the peaks should be unchanged.
[63] C. Karolis and E. Harting, J. Phys. B **11**, 357 (1978).
[64] G. K. James, J. M. Ajello, and W. R. Pryor, J. Geophys. Res. **103**, 20113 (1998).
[65] A. Aguilar, J. M. Ajello, R. S. Mangina, G. K. James, H. Abgrall, and E. Roeuff, Astrophys. J., Suppl. Ser. **177**, 388 (2008).
[66] B. P. Lavrov, A. S. Melnikov, M. Käning, and J. Röpcke, Phys. Rev. E **59**, 3526 (1999).
[67] U. Fantz, B. Schalk, and K. Behringer, New J. Phys. **2**, 7 (2000).
[68] B. Van Zyl and H. Neumann, J. Geophys. Res. **85**, 6006 (1980); B. Van Zyl, M. W. Gealy, and H. Neumann, Phys. Rev. A **28**, 176 (1983).
[69] B. M. Jelenković and A. V. Phelps, in *Swarm Studies and Inelastic Electron-Molecule Collisions*, edited by L. C. Pitchford, B. V. McCoy, A. Chutjan, and S. Trajmar (Springer-Verlag, New York, 1985), p. 113; this work with D_2 found ~10% distortion of the spatial distribution of emission when the current was raised to 10 μA. Because of higher ion drift velocities in H_2, the distortion for H_2 discharges is expected to become noticeable for higher currents than for D_2.
[70] S. J. B. Corrigan and A. von Engel, Proc. R. Soc. London, Ser. A **245**, 335 (1958).
[71] F. Llewellyn Jones, Handb. Phys. **22**, 1 (1956).
[72] V. O. Stern and M. Volmer, Phys. Z. **20**, 183 (1919).
[73] A. Catherinot, B. Dubreuil, and M. Gand, Phys. Rev. A **18**, 1097 (1978).
[74] J. Bittner, K. Kohse-Höinghaus, U. Meier, and Th. Just, Chem. Phys. Lett. **143**, 571 (1988).
[75] B. L. Preppernau, K. Pearce, A. Tserepi, E. Wurzberg, and T. A. Miller, Chem. Phys. **196**, 371 (1995).
[76] K. Niemi, V. Schulz-von der Gathen, and H. F. Döbele, J. Phys. D **34**, 2330 (2001); A. Francis, T. Gans, K. Niemi, U. Czarnetzki, V. Schulz-von der Gathen, and H. F. Döbele, Proc. SPIE **4460**, 122 (2002).
[77] E. U. Condon and G. H. Shortley, *The Theory of Atomic Spectra* (Cambridge University Press, Cambridge, England, 1967), p. 137.
[78] H. A. Bethe and E. E. Saltpeter, *Quantum Mechanics of One- and Two-Electron Atoms* (Academic, New York, 1957), p. 284.
[79] C. C. Havener, N. Rouze, W. B. Westerveld, and J. S. Risley, Phys. Rev. A **33**, 276 (1986).
[80] R. H. Hughes and H. Kisner, Phys. Rev. A **5**, 2107 (1972).
[81] B. M. Jelenković and A. V. Phelps (unpublished).
[82] J. Phillips, C. K. Chen, and R. L. Mills, Int. J. Hydrogen Energy **33**, 2419 (2008); the relative Balmer line intensities shown in Fig. 6(b) of this reference are in very good agreement with the values shown by the various sets of data in Fig. 2 of the present paper. This means that the apparent electron excitation temperature derived by Phillips *et al.* is most probably not a measure of the energy of the low density of plasma electrons but is the result of excitation of H_2 by electrons and/or fast H atoms produced in a rf discharge sheath with average energies on the order of 100 eV. The lack of knowledge as to the plasma conditions at the point of production of the radiation observed by Phillips *et al.* prevents further analysis.
[83] G. R. Möhlmann, S. Tsurubuchi, and F. J. De Heer, Chem. Phys. **18**, 145 (1976).
[84] G. A. Baraff and S. J. Buchsbaum, Phys. Rev. **130**, 1007 (1963).
[85] A. B. Wedding and A. V. Phelps, J. Chem. Phys. **89**, 2965 (1988).

[86] A plot of our continuum emission data at various pressures extrapolated to the anode similar to that of Fig. 6 also shows that the effect of quenching is small compared to the scatter.
[87] The expected improved signal to noise level was only partially realized because of unstable operation of the discharge at the time of the near-uv measurements.
[88] G. Dieke, in *The Hydrogen Molecule Wavelength Tables Of Gerhard Heinrich Dieke*, edited by H. M. Crosswhite (Wiley-Interscience, New York, 1972).
[89] D. R. Schultz, P. S. Krstic, T. Minami, M. S. Pindzola, F. J. Robicheaux, J. P. Colgan, S. D. Loch, D. C. Griffin, C. P. Ballance, N. R. Badnell, and H. P. Summers, Contrib. Plasma Phys. **44**, 247 (2004).
[90] V. D. Stojanović, B. M. Jelenković, and Z. Lj. Petrović, J. Appl. Phys. **81**, 1601 (1997); see also Ref. [26].
[91] Z. Lj. Petrović, V. D. Stojanović, and Z. D. Nikitović, in *VI Serbian Conference on Spectral Line Shapes in Astrophysics*, edited by L. Č. Popović and M. S. Dimitrijević, AIP Conf. Proc. No. 938 (AIP, New York, 2007), p. 237.
[92] S. Miller, T. Stallard, C. Smith, G. Millward, H. Melin, M. Lystrup, and A. Aylward, Philos. Trans. R. Soc. London, Ser. A **364**, 3121 (2006).
[93] C. B. Kerkdijk, C. M. Smits, D. R. Olander, and F. W. Saris, Surf. Sci. **49**, 45 (1975).
[94] Yu-Yuan R. Hsiao and R. C. Amme, Phys. Rev. A **20**, 214 (1979).
[95] A. V. Phelps, Bull. Am. Phys. Soc. **53**, 41 (2008).